22 Fluorophore-Conjugated Chimeric Anti-CEA Antibodies for Fluorescence-Guided Surgery of Gastrointestinal (GI) Tumors

Michael Bouvet and Robert M. Hoffman

Introduction

The ability of the surgeon to accurately visualize tumor margins and identify metastases is necessary for the success of cancer surgery. Fluorescence optical imaging, because of its high sensitivity, low cost, portability, and real-time capabilities, has great potential to improve surgical outcomes.

Fluorescence technology have already been used clinically. Frangioni et al. carried out the first-in-human clinical trial of fluorescent imaging in breast cancer sentinel lymph node mapping using indocyanine green (ICG) as a near-infrared (NIR) fluorescent lymphatic tracer [1]. Van Dam et al. used folate conjugated to fluorescein isothiocyanate for targeting folate receptor alpha (FR-α) in patients with ovarian tumors [2]. Fluorescence was detectable intraoperatively in all patients with a malignant tumor.

M. Bouvet, M.D. (✉)
Department of Surgery, Moores UCSD Cancer Center, 3855 Health Science Drive #0987, La Jolla, CA 92093-0987, USA
e-mail: mbouvet@ucsd.edu

R.M. Hoffman, Ph.D.
AntiCancer, Inc., 7917 Ostrow Street, San Diego, CA 92111, USA

Department of Surgery, University of California San Diego, 3855 Health Science Drive #0987, La Jolla, CA 92093-0987, USA
e-mail: all@anticancer.com

In preclinical studies, Tsien et al. used activatable cell-penetrating peptides (ACPPs), in which the fluorescently-labeled, polycationic cell-penetrating peptide (CPP) is coupled via a cleavable linker to a neutralizing peptide. Upon exposure to tumor proteases surgery, the linker is cleaved, dissociating the inhibitory peptide and allowing the CPP to bind to and enter tumor cells [3]. Kishimoto et al. selectively labeled tumors with a genetic reporter, GFP, using a telomerase-dependent adenovirus genetic OBP-401 [4]. They demonstrated that tumors recurred after fluorescence-guided surgery and maintained GFP expression [5]. Therefore, the detection of recurrence and future metastasis is possible with OBP-401 GFP labeling, since recurrent cancer cells stably express GFP, which is not possible with nongenetic labeling of tumors.

Negative tumor margins are especially necessary for curative pancreatic cancer surgery, For colorectal cancers the high mortality of this disease in the United States correlates with a high cancer incidence [6]. Colon cancer patients more often present with resectable disease [7] and have more surgical options than patients with pancreatic cancer [8, 9]. There is a clear advantage to compete resection of all primary and metastatic cancer at the time of surgery of colon cancer when clinically appropriate [10, 11].

Monoclonal antibodies specific for either CA19-9 or CEA were conjugated to a green fluorophores delivered to pancreatic or colon cancer-bearing mice as a single intravenous dose [12–18]. Using fluorescence imaging, the primary pancreatic

F.D. Dip et al. (eds.), *Fluorescence Imaging for Surgeons: Concepts and Applications*,
DOI 10.1007/978-3-319-15678-1_22, © Springer International Publishing Switzerland 2015

or colon tumor was clearly visible at laparotomy as were small metastases in other organs.

The present chapter reviews the potential of using chimeric mouse-human antibodies conjugated with appropriate fluorophores for fluorescence-guided surgery (FGS) of metastatic pancreatic and colon cancer in orthotopic nude mouse models. The possibility of this technology to change the paradigm for surgical oncology is also discussed.

Carcinoembryonic Antigen

Carcinoembryonic antigen (CEA) was first described following immunization of xenogenic animals with human tumor tissue [19]. Human tissue specimens were positive for CEA expression from multiple cancers arising from endodermally-derived epithelium of the digestive tract [20] as well as in the human embryonic gut, pancreas, and liver tissue [21]. Although initially identified in adenocarcinoma of the colon [20], CEA is often also expressed in pancreatic ductal adenocarcinoma [22, 23].

CEA is considered is an oncofetal antigen, with expression in normal fetal tissues but only has a trace presence in normal adult human tissue [24, 25]. The CEA family is comprises a large class of complex glycoproteins of the immunoglobulin gene superfamily [26]. In addition to acting as a marker for human gastrointestinal cancers, CEA also functions as an intercellular adhesion molecule and may have some immunoregulatory function as well [27]. In clinical medicine, CEA is most commonly utilized as a serum marker in colorectal and pancreatic cancer for preoperative staging and follow-up of patient response outcome after surgery and chemotherapy [28, 29].

In Vitro Expression of CEA

In vitro, 70 % of the pancreatic cancer cell lines tested were positive for CEA immunostaining in culture. CEA-positive pancreatic cancer cell lines included MiaPaca-2, FG, ASPC-1, BxPC-3, CFPAC, Panc-1, and Capan-1. The cell lines tested that did not express CEA included XPA-1, XPA-3, and XPA-4. Of the human colon cancer cell lines that were tested in vitro, 67 % expressed CEA as identified by immunostaining. The CEA-positive colon cancer cell lines included LOVO, HCT-116, SW948, and LS174T. The colon cancer cell lines that did not express CEA were HT-29 and SW480. For each cell line tested, the cells were incubated with Alexa Fluor 488-labeled anti-CEA or IgG. Positive staining was indicated by fluorescence intensity above background staining with conjugated non-specific IgG (Table 22.1) [12].

Immunofluorescence Staining of Tissue for Binding with Anti-CEA Antibody

Screening of normal human tissue samples for binding to conjugated anti-CEA antibody used immunofluorescence staining of a human tissue array. This array contained two samples each of 19 different noncancerous adult human tissues including: salivary gland, liver, small intestine, stomach, kidney, skeletal muscle, skin, heart, placenta, breast, cervix, uterus, spleen, lung, brain, thyroid, pancreas, ovary, and adrenal gland. Human tumor grown in nude mice from the pancreatic cancer cell line ASPC-1 and the primary human colon cancer tumor Colo4104 were used as positive controls, and mouse axillary lymph node tissue was included as a negative control. Both the ASPC-1 pancreatic tumor and the Colo4104 colon tumor yielded positive staining for CEA. In noncancerous tissues the majority of samples did not demonstrate binding of conjugated anti-CEA above the isotype-control IgG background. A low level of staining above background was present within the small intestine and cervix. Notably, the normal colon and pancreas did not bind conjugated anti-CEA. Table 22.2 denotes the staining for all noncancerous human lists samples tested [12].

Table 22.1 CEA expression in vitro and in vivo

Human pancreatic cancer cell lines		
In vitro	+	–
Mia Paca-2	x	
FG	x	
BxPC-3	x	
CFPAC	x	
Panc-1	x	
Capan-1	x	
XPA-1		x
XPA-3		x
XPA-4		x
In vivo	+	–
ASPC-1	x	
BxPC-3	x	
CFPAC	x	
Panc-1	x	
Capan-1	x	
Human colon cancer cell lines		
In vitro	+	–
LOVO	x	
HCT-116	x	
SW948	x	
LS174T	x	
HT-29		x
SW480		x
In vivo	+	–
LS174T	x	
Colo4104	x	

Human pancreatic and colon cancer cell lines were tested for in vitro and in vivo expression of CEA and seven of ten (70 %) were positive. Four of 6 (67 %) colon cancer cell were positive. All seven pancreatic cancer cell lines and one colon cancer cell line tested in vivo positive. In addition, the primary patient human colon cancer tissue Col4104, grown in mice, was also positive [11].

Table 22.2 CEA expression in adult human tissues

Tissue	Staining
Salivary gland	–
Liver	–
Small intestine	+/–
Stomach	–
Kidney	–
Skeletal muscle	–
Skin	–
Heart	–
Placenta	–
Breast	–
Cervix	+
Uterus	–
Spleen	–
Lung	–
Brain	–
Thyroid	–
Pancreas	–
Ovary	–
Adrenal gland	–
ASPC-1 tumor[a]	+++
Colo4104 tumor[a]	++
Mouse axillary LN[b]	–

Staining of a tissue array of adult noncancerous human tissues demonstrated only a small amount of positive staining over background in cervix and small intestine tissues. In the small intestine, staining was primarily limited to cells on the mucosal surface. In the cervix, the staining was primarily on the luminal surface of glandular structures. The positive controls ASPC-1 and Colo4104 stained with conjugated anti-CEA both within the cytoplasm and on the cell membrane [11].

[a]Positive control

[b]Negative control

Fluorophore-Conjugated Anti-A Antibody for the Intraoperative Imaging and FGS of Pancreatic and Colorectal Cancer

In 2008, our team was the first to evaluate the use of a fluorophore-labeled anti-CEA monoclonal antibody to aid in primary and metastatic cancer visualization and FGS in nude mouse models of human colorectal and pancreatic cancer [12]. Anti-CEA conjugated with a green fluorophore, resulted in improved resection. Subcutaneous, orthotopic primary and metastatic human pancreatic and colorectal tumors were readily visualized with fluorescence imaging after administration of conjugated anti-CEA. The fluorescence signal was detectable 30 min after systemic antibody delivery and was stable for 2 weeks, with minimal in vivo photobleaching after exposure to standard operating room lighting. We demonstrated the principle that fluorophore-conjugated antibodies enabled successful FGS in orthotopic mouse models of pancreatic cancer [17].

Imaging of Subcutaneous Tumors with Fluorescent Anti-CEA Antibody

The human pancreatic cancer cell lines ASPC-1, BxPC-3, CFPAC, Panc-1, and Capan-1 were implanted subcutaneously in nude mice and evaluated for CEA expression. One colon cancer cell line (LS174T) and a primary human colon cancer patient specimen (Colo4104) , grown in nude mice, were also implanted subcutaneously. When the tumors had reached approximately 1–2 mm diameter, the animals were each given a single dose of Alexa Fluor 488-conjugated anti-CEA or IgG i.v. All 5 pancreatic cancer cell lines implanted bound the CEA as did the colon cancer cell line as well as the patient colon cancer model demostrated by fluorescence intensity above background IgG (Table 22.1).

Imaging Orthotopic Tumors with Fluorescent Anti-CEA Antibody

Tumors implanted orthotopically into the nude mouse pancreas and colon were evaluated for imaging using conjugated anti-CEA. The human pancreatic cancer cell lines ASPC-1 and BxPC-3 were used. For the colon cancer, the patient tumor Colo4014 was used in a model termed patient-derived orthotopic xenograft (PDOX®) [30, 31]. Orthotopic pancreatic or colon tumor-bearing mice were given a single dose of Alexa Fluor 488-conjugated anti-CEA or IgG via tail vein injection 7–10 days after tumor implantation. The animals were imaged under both bright field and fluorescence illumination using the Olympus variable-magnification OV100 Small Animal Imaging System [32]. Intravital fluorescence imaging revealed very small ASPC-1 and BxPC-3 tumors which were not visible under bright-field illumination, even at higher magnification (Fig. 22.1a–c). With fluorescence imaging it was clear that the extent of tumor invasion was much greater than that seen under standard bright light (Fig. 22.1d, e). The tumors in the colon cancer-bearing animals were visible under both bright field and fluorescence imaging at the magnification used (Fig. 22.2a–e). The animals which received control conjugated IgG had no green fluorescence in either their pancreatic (Fig. 22.1a, b) or colon (Fig. 22.2a, b) tumors [12].

Imaging Intra-abdominal Disseminated Tumor with Fluorescent Anti-CEA Antibody

Mouse models of intra-abdominal carcinomatosis of pancreatic and colorectal cancer were used to evaluate fluorophore-conjugated anti-CEA binding to these tumors in vivo. Animals were injected i.p. with human pancreatic (BxPC-3) or colorectal (Colo4104 or LS174T) cancer cells. After 1 week the mice were given a single 75 μg injection of Alexa Fluor 488-conjugated anti-CEA or IgG i.v. The mice were imaged 24 h later with the Olympus OV100 using both bright field and fluorescence illumination. At the time of imaging, these animals had very small peritoneal implants on the bowel and mesentery which were difficult to visualize using bright field imaging (Figs. 22.3a, b and 22.4a, b) but were very clearly visible under fluorescence illumination in mice given conjugated anti-CEA (Figs. 22.3c, d and 22.4c, d). The mice which received IgG had no visible fluorescence signal in their tumors (data not shown) [12].

Time-Course Imaging of Pancreatic Tumors in Nude Mice After Injection of Fluorescent Anti-CEA Antibody

Time-course imaging of human pancreatic tumors in nude mice labeled with conjugated anti-CEA demonstrated rapid binding of the antibody-fluorophore conjugate in vivo with very long signal duration. Mice with 1–2 mm diameter subcutaneous ASPC-1 tumors were given a single dose of Alexa Fluor 488-conjugated anti-CEA i.v. The mice were then imaged over 15 days after delivery of a single dose of

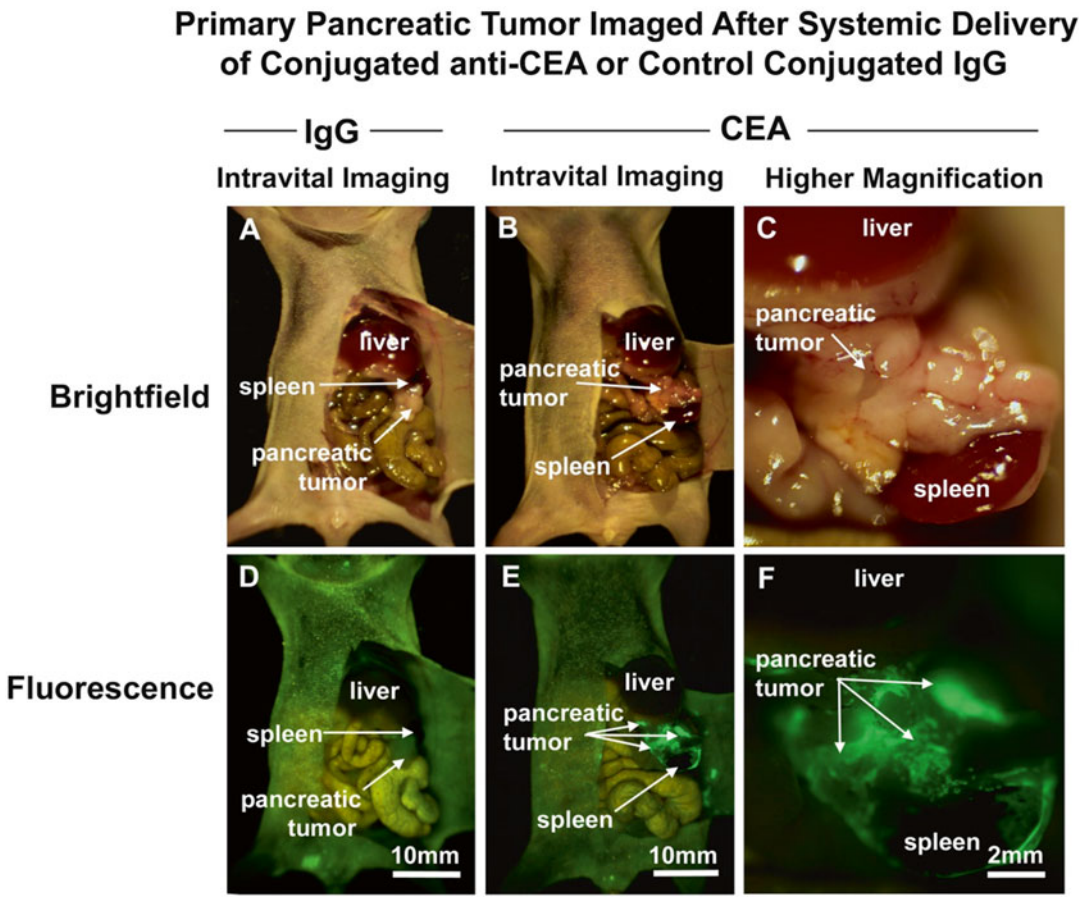

Fig. 22.1 Imaging of orthotopic human pancreas tumors in vivo had greatly improved primary tumor visualization at laparotomy. After treatment with fluorophore conjugated anti-CEA, mice with orthotopically-implanted BxPC-3 pancreatic tumors were imaged using both bright field (**a**–**c**) and fluorescence (**d**–**f**) illumination. Primary tumors were difficult to clearly distinguish under bright field imaging under both low (**a**, **b**) and high (**c**) magnification. In contrast, fluorescence illumination of anti-CEA-labeled tumors enabled identification of primary tumor (**e**, **f**), which was much more extensive than seen under bright field. Animals given conjugated non-specific IgG demonstrated no fluorescence signal in the orthotopic tumor (**d**). All tumors was confirmed by histology [12]

antibody. Two animals were imaged for each time point. A small amount of fluorescence signal could be seen at 30 min post-antibody injection, and the signal peaked at 24 h. This signal was stable over the next 24 h and then decreased over the following 6 days decaying to a low-level signal at 8 days post-injection. By 15 days there was undetectable signal remaining within the tumor tissue (Fig. 22.5) [12].

Use of Fluorescent Anti-CEA Antibody to Image Post-resection Residual Tumor

In animals bearing larger (3–10 mm diameter) subcutaneous tumors, we used fluorophore-conjugated anti-CEA to attempt a complete resection. Mice were given a single dose of Alexa Fluor 488-conjugated anti-CEA 24 h prior to

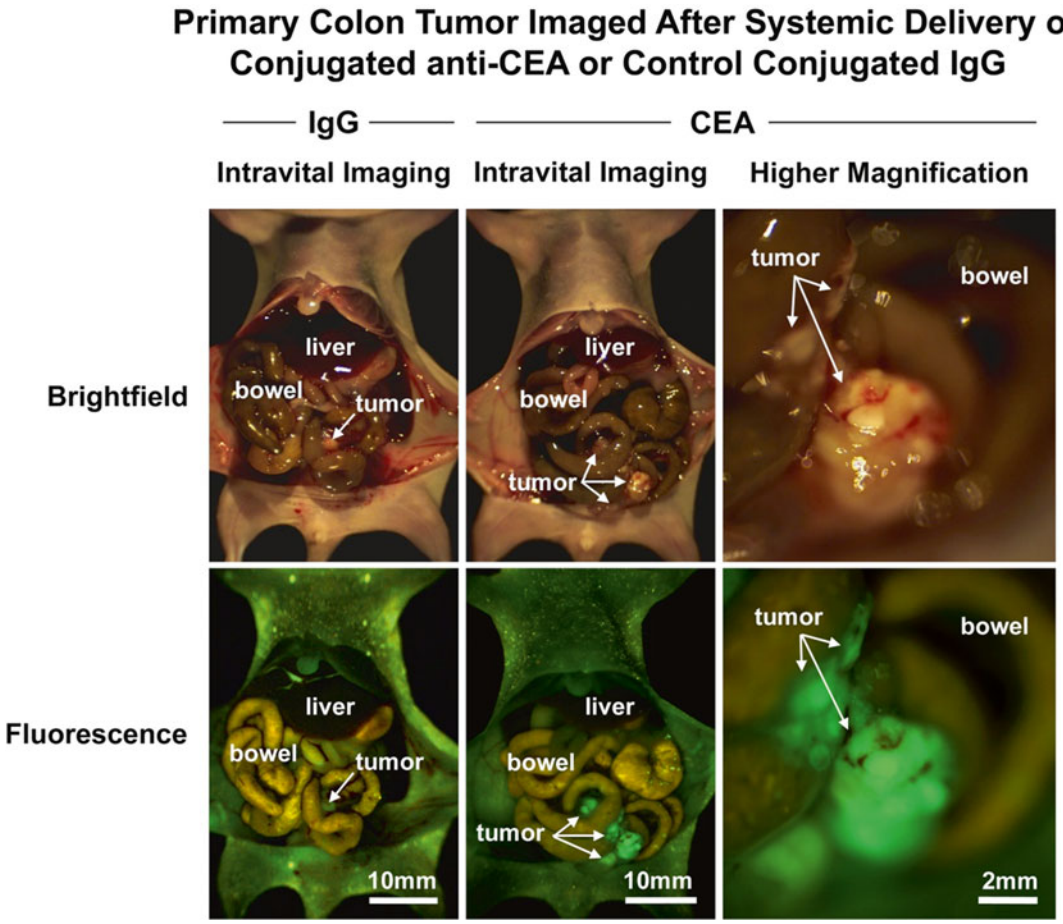

Fig. 22.2 Fluorescence imaging of patient-derived orthotopic xenograft (PDOX®) human colon tumors under fluorescence illumination improved primary tumor visualization at laparotomy. Mice with orthotopically-implanted low-passage AC4104 colon tumors originally derived from a patient were imaged under both bright field (**a**–**c**) and fluorescence (**d**–**f**) illumination. Primary tumors labeled with conjugated anti-CEA had bright green fluorescence (**e**, **f**). Mice given conjugated control IgG had no fluorescence signal in the orthotopic tumor (**d**). All tumors were confirmed by histology [12]

FGS. Before surgery, animals were anesthetized, and their tumors were imaged using bright field and fluorescence illumination (Fig. 22.6a, b). The tumors were then carefully resected with a dissecting microscope under bright field illumination with careful attention paid to removing all visible tumor tissue without adjacent normal skin or muscle (Fig. 22.6b–d). Following resection the operative bed was then imaged using fluorescence microscopy, with all remaining areas of fluorescence (Fig. 22.6e, f) were documented and biopsied. Of the three animals that underwent bright light surgery (BLS), all three had residual tumor present within the tumor bed which was not visible under bright field illumination. The presence of all tumor tissue was confirmed by histology (data not shown) [12].

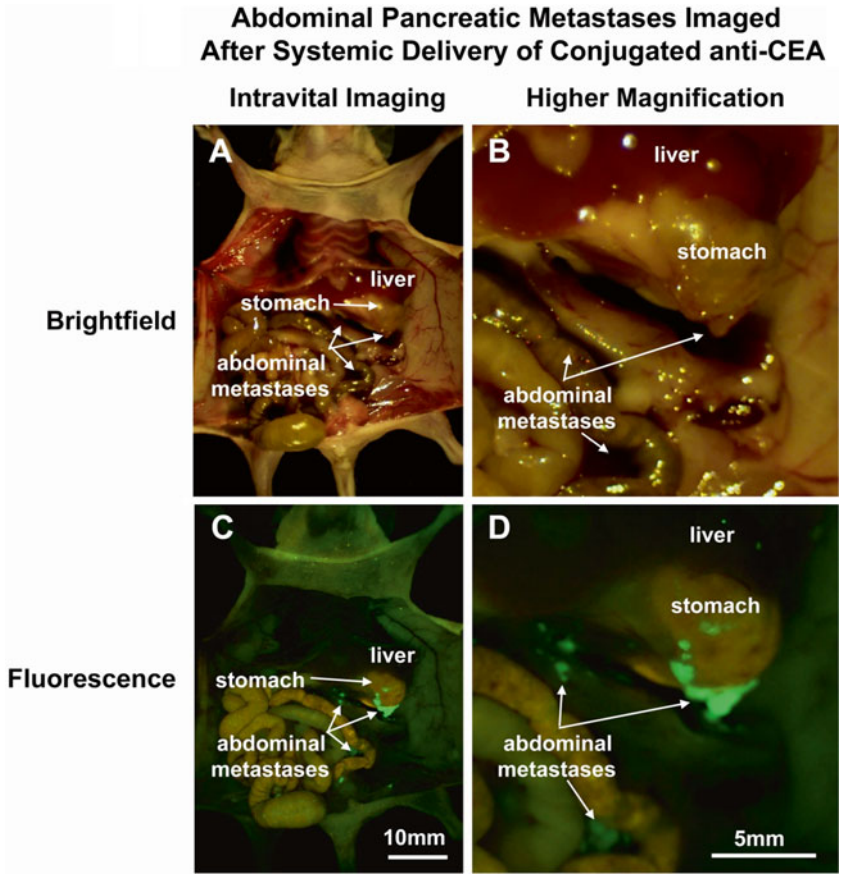

Fig. 22.3 Fluorescence imaging of intra-abdominal metastases from human pancreatic cancer cell line BxPC-3 orthotopic models reveals greatly improved metastatic tumor visualization at laparotomy. Mice injected i.p. with BxPC-3 pancreatic cancer cells, were imaged using in bright field (**a**, **b**) and under fluorescence (**c**, **d**) illumination. Small metastatic implants on the bowel and mesentery were not seen with bright field imaging even under low (**a**) or high (**b**) magnification. In contrast, fluorescence illumination of anti-CEA-labeled tumors enabled easy identification of metastases (**c**, **d**) [12]

FGS with a Fluorophore-Conjugated Anti-CEA Antibody Improves Surgical Resection and Increases Survival in Orthotopic Mouse Models of Human Pancreatic Cancer

We showed that FGS with anti-CEA antibody conjugated to a green fluorophore improved outcomes in mouse models of pancreatic cancer [17]. Mouse models of human pancreatic cancer were established with surgical orthotopic implantation (SOI) of the human BxPC-3 pancreatic cancer cell line. Orthotopic tumors were allowed to develop for 2 weeks and the mice then underwent BLS or FGS 24 h after intravenous injection of anti-CEA-Alexa 488. Completeness of resection was assessed from postoperative fluorescence imaging. Mice were followed postoperatively to determine disease-free survival (DFS) and overall survival (OS). Complete resection was achieved in 92 % of FGS-treated mice as compared to 45.5 % in the BLS group ($p=0.001$). FGS resulted in a smaller postoperative tumors ($p=0.01$). Cure rates with FGS compared to BLS improved from 4.5 to 40 % ($p=0.01$). One year postoperative survival rates increased from 0 % with BLS to 28 % with FGS ($p=0.01$). Median DFS improved from 5 weeks with BLS to 11 weeks

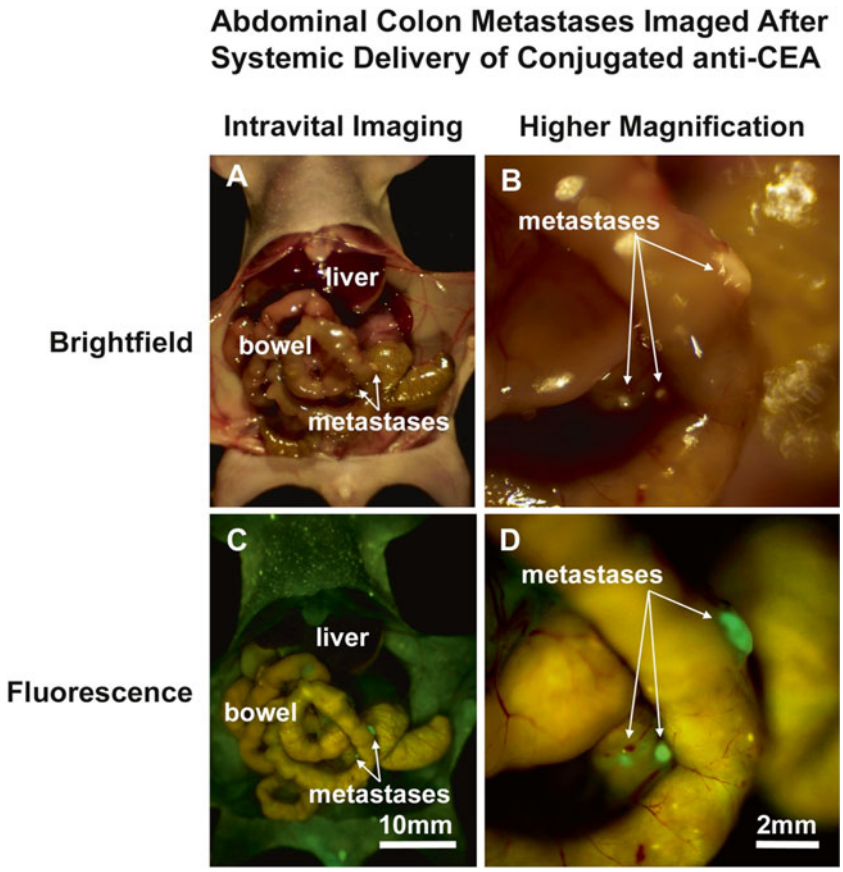

Fig. 22.4 Mice with metastatic human colon tumors had improved tumor visualization at laparotomy after injection of fluorophore-conjugated chimeric anti-CEA antibodies. Mice with intraperitoneally implanted Colo4104 colon cancer were imaged using both bright field (**a**, **b**) and fluorescence (**c**, **d**) illumination. The metastases were difficult to distinguish under bright field imaging under both low (**a**) and high (**b**) magnification. In contrast, fluorescence illumination of anti-CEA-labeled tumors enabled facile identification of metastases (**c**, **d**) [12]

with FGS ($p=0.0003$). Median OS improved from 13.5 weeks with BLS to 22 weeks with FGS ($p=0.001$) (Fig. 22.7) [17].

Fluorescently Labeled Chimeric Anti-CEA Antibody Improves Detection and Resection of Human Colon Cancer in a Patient-Derived Orthotopic Xenograft (PDOX®) Nude Mouse Model

A fluorescently labeled chimeric anti-CEA antibody improved detection and FGS of colon cancer [16]. Mouse monoclonal antibodies tend to evoke an immune reaction when administered to humans. Creating a chimeric "fusion" protein allows the introduction of segments of human constant domains while maintaining important properties from the "parent" mouse protein, thereby eliminating most of the potentially immunogenic portions of the antibody without compromising its specificity for the intended target (Fig. 22.8) [33]. Frozen tumor and normal human tissue samples were stained with chimeric and mouse antibody-fluorophore conjugates for comparison of tumor staining. PDOX® mice with human colon cancer underwent FGS or BLS 24 h after i.v. injection of fluorophore-conjugated chimeric anti-CEA

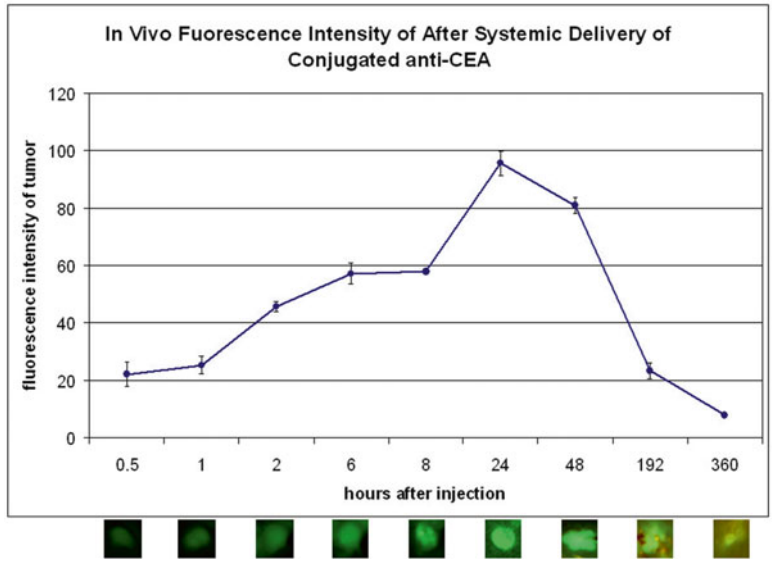

Fig. 22.5 Mice with small subcutaneous tumors were given a single dose of conjugated antibody and imaged at 30 min, 1 h, 2 h, 6 h, 8 h, 24 h, and 48 h and 8 and 15 days after. The fluorescence signal was detected at 30 min and peaked at 24 h after injection. The fluorescence signal remains high at 48 h but by 8 days (192 h) decayed to levels comparable to that seen at 30 min and by 15 days (360 h) was at background [12]

antibody. Completeness of resection was assessed using postoperative imaging. Mice were followed for 6 months to determine recurrence. The fluorophore conjugation efficiency (dye/mole ratio) improved from 3–4 to >5.5 with the chimeric anti-CEA antibody compared to mouse anti-CEA antibody. CEA-expressing tumors labeled with chimeric CEA antibody had a brighter fluorescence signal on frozen human tumor tissues ($p = 0.046$). Normal human tissues had lower fluorescence with chimeric anti-CEA compared to mouse antibody. Chimeric CEA antibody accurately labeled PDOX® colon cancer in nude mice, enabling more effective FGS. The R0 resection rate improved from 86 to 96 % with FGS compared to BLS (Fig. 22.9).

Comparison of a Chimeric Anti-CEA Antibody Conjugated with Visible or Near-Infrared Fluorescent Dyes for Imaging Pancreatic Cancer in Orthotopic Nude Mouse Models

We evaluated a set of visible and near-infrared dyes conjugated to a tumor-specific chimeric antibody for their ability to improve high-resolution tumor imaging in orthotopic models of pancreatic cancer [14]. BxPC-3 human pancreatic cancer was orthotopically implanted into the pancreata of nude mice. The orthotopic models received a single i.v. injection of a chimeric anti-CEA antibody conjugated to one of the following fluorophores: the 488 nm group (Alexa Fluor 488 or DyLight 488),

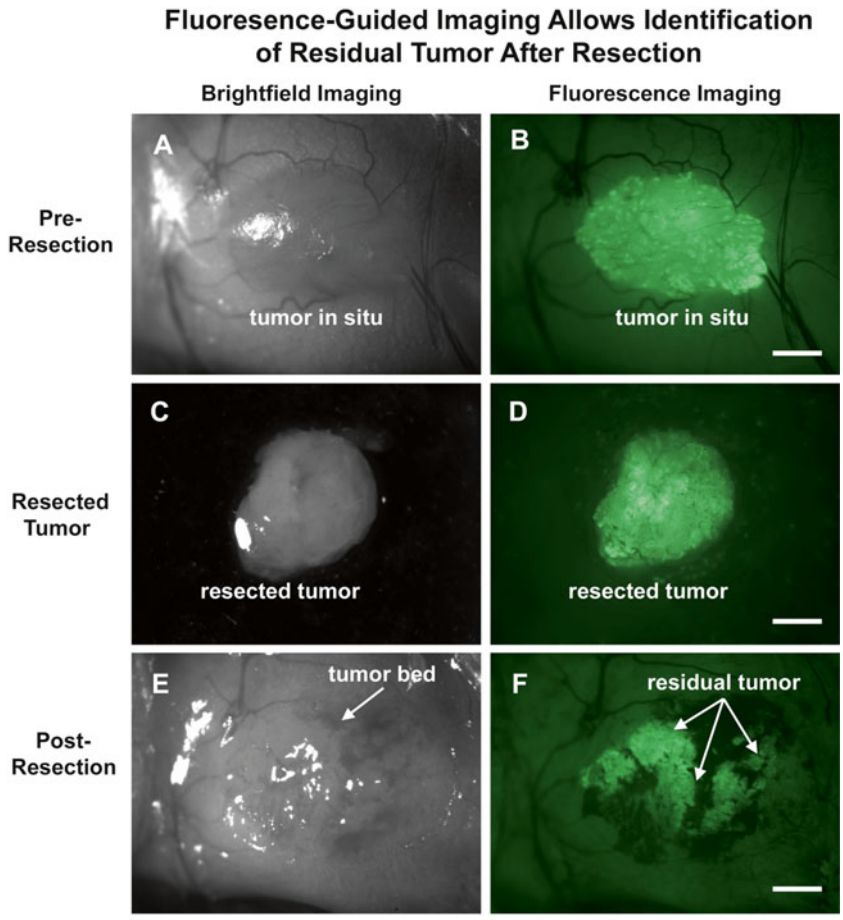

Fig. 22.6 Tumor resection under bright-light microscopy. Larger subcutaneous BxPC-3 tumors were imaged under a dissecting microscope via both bright field (**a**) and fluorescence (**b**) illumination. Under bright field microscopy, all visible tumor was resected, and the ex vivo tumor was imaged under bright field (**c**) and fluorescence (**d**) microscopy. The tumor resection bed (**e**) was then imaged under fluorescence microscopy for any evidence of residual fluorescence (**f**). In all animals resected, there was residual cancer cells visualized under fluorescence within the tumor bed. Resected and residual tumor was confirmed tumor by histology. All images taken at 20×, scale bars = 1 mm [12]

550 nm group (Alexa Fluor 555 or DyLight 550), 650 nm group (Alexa Fluor 660 or DyLight 650), and 750 nm group (Alexa Fluor 750 or DyLight 755). Twenty-four hours later, the Olympus OV100 small animal imaging system was used to compare the various dyes conjugated to anti-CEA for depth of imaging, resolution, tumor to background ratio, photobleaching, and hemoglobin quenching. The longer-wavelength dyes effected increased depth of penetration and ability to detect the smallest tumor deposits and provided the highest tumor to background ratios, resistance to hemoglobin quenching, and increased tumor specificity (Fig. 22.10). The shorter-wavelength dyes were more photostable [14].

Future Directions of Fluorescence-Guided Surgery and Fluorescence Laparoscopy

Fluorophore-conjugated tumor specific antibodies enabled labeling, detection, and subsequently FGS to improve surgical outcomes in mouse

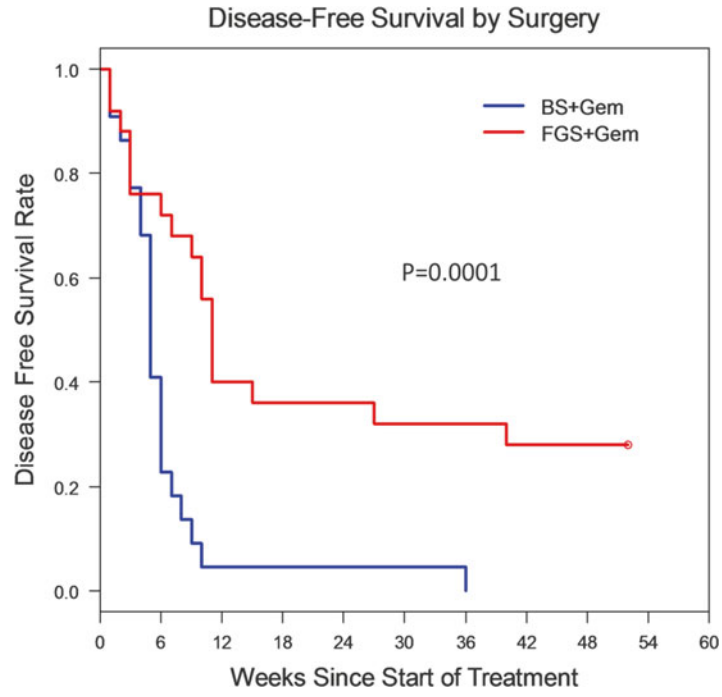

Fig. 22.7 Disease-free survival after FGS using a fluorophore-conjugated anti-CEA antibody in orthotopic mouse models of human pancreatic cancer. There was a significant improvement in disease-free survival with FGS compared to BLS ($p < 0.0001$). Mice with the FGS group had a median disease-free survival of 11 weeks compared to 5 weeks with BLS [17]

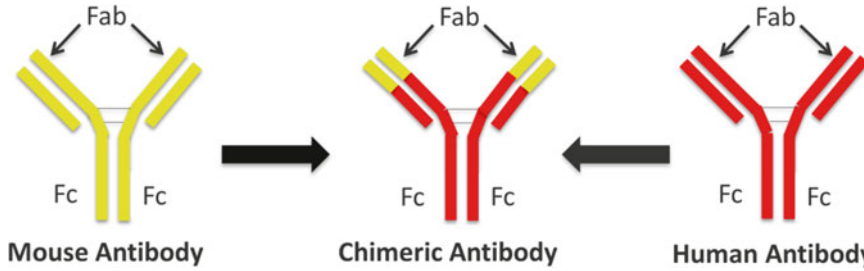

Fig. 22.8 Process of chimerization of anti-CEA antibody. This diagram represents the process of making a mouse-human chimeric anti-CEA antibody (Aragen Bioscience, Inc.) [16]

models of pancreatic and colon cancer. FGS significantly reduced the postoperative tumor burden in the recurrence. The improved R0 resection rate resulted in longer disease-free survival and overall survival. Fluorophore-conjugated antibodies were also be used to detect GI cancers using minimally invasive fluorescence laparoscopy [15, 18, 34].

The goal is to improve all methods of fluorescently labeling tumor and metastases for curative FGS. It is necessary to sterilize the tumor bed after FGS of all residual cancer cells using UVC irradiation, intraoperative chemotherapy, or photoimmunotherapy.

Conclusions

In this chapter, we have reviewed the use of a fluorophore-antibody conjugates specific for the oncofetal antigen CEA to effectively image both primary and metastatic colon and pancreatic tumors in clinically relevant orthotopic mouse models. This approach offers the advantage of a

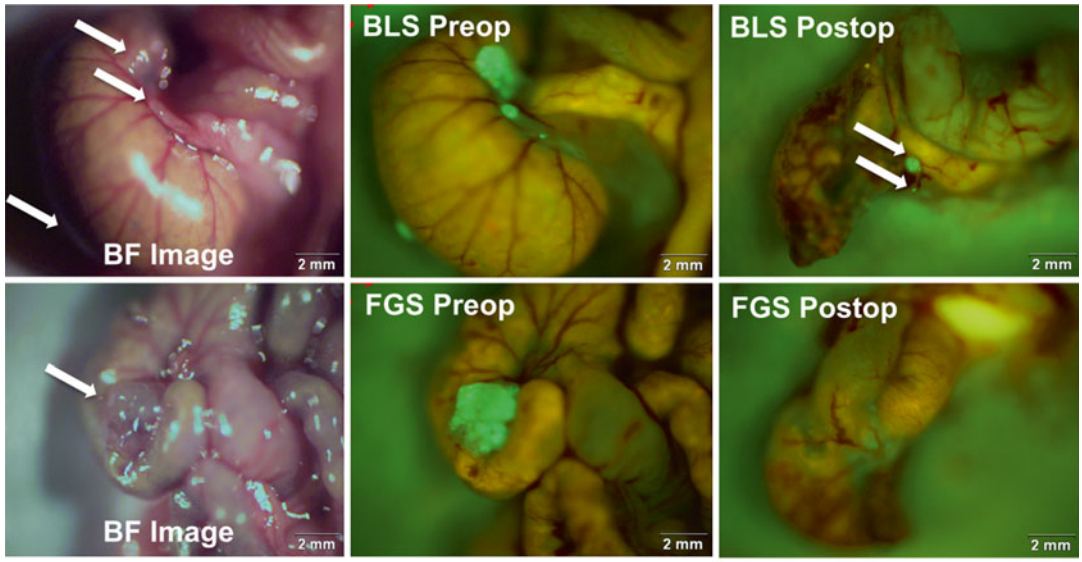

	BLS	FGS
Complete Resection Rate	85.7% (18/21)	95.5% (21/22)

Fig. 22.9 FGS with fluorophore-conjugated chimeric antibody improved real-time detection of tumor margins, thereby increasing complete resections with FGS-compared to BLS-treated mice from 85.7 % to 95.5 %, respectively. Small tumor deposits (indicated by *white arrows*) remained after BLS. The absence of any fluorescence signal in the mouse after FGS indicates complete resection. The preoperative bright field images are on the left to better illustrate the difficulty of identifying tumor margins without fluorescence labeling. *White arrows* indicate tumor lesions in the wall of the cecum [16]

single antibody delivery which improved the identification of residual tumor tissue at the time of resection thereby enabling FGS which significantly improved tumor resection, decreased recurrence, and lengthened overall survival.

Acknowledgment Work supported in part by grants from the National Cancer Institute CA142669 and CA132971 (to M.B. and AntiCancer, Inc.).

References

1. Troyan SL, Kianzad V, Gibbs-Strauss SL, Gioux S, Matsui A, Oketokoun R, et al. The FLARE intraoperative near-infrared fluorescence imaging system: a first-in-human clinical trial in breast cancer sentinel lymph node mapping. Ann Surg Oncol. 2009;16(10):2943–52.
2. van Dam GM, Themelis G, Crane LM, Harlaar NJ, Pleijhuis RG, Kelder W, et al. Intraoperative tumor-specific fluorescence imaging in ovarian cancer by folate receptor-alpha targeting: first in-human results. Nat Med. 2011;17(10):1315–9.
3. Nguyen QT, Olson ES, Aguilera TA, Jiang T, Scadeng M, Ellies LG, et al. Surgery with molecular fluorescence imaging using activatable cell-penetrating peptides decreases residual cancer and improves survival. Proc Natl Acad Sci U S A. 2010;107(9):4317–22.
4. Kishimoto H, Zhao M, Hayashi K, Urata Y, Tanaka N, Fujiwara T, et al. In vivo internal tumor illumination by telomerase-dependent adenoviral GFP for precise surgical navigation. Proc Natl Acad Sci U S A. 2009;106(34):14514–7.
5. Kishimoto H, Aki R, Urata Y, Bouvet M, Momiyama M, Tanaka N, et al. Tumor-selective, adenoviral-mediated GFP genetic labeling of human cancer in the live mouse reports future recurrence after resection. Cell Cycle. 2011;10(16):2737–41.
6. Siegel R, Naishadham D, Jemal A. Cancer statistics, 2013. CA Cancer J Clin. 2013;63(1):11–30.

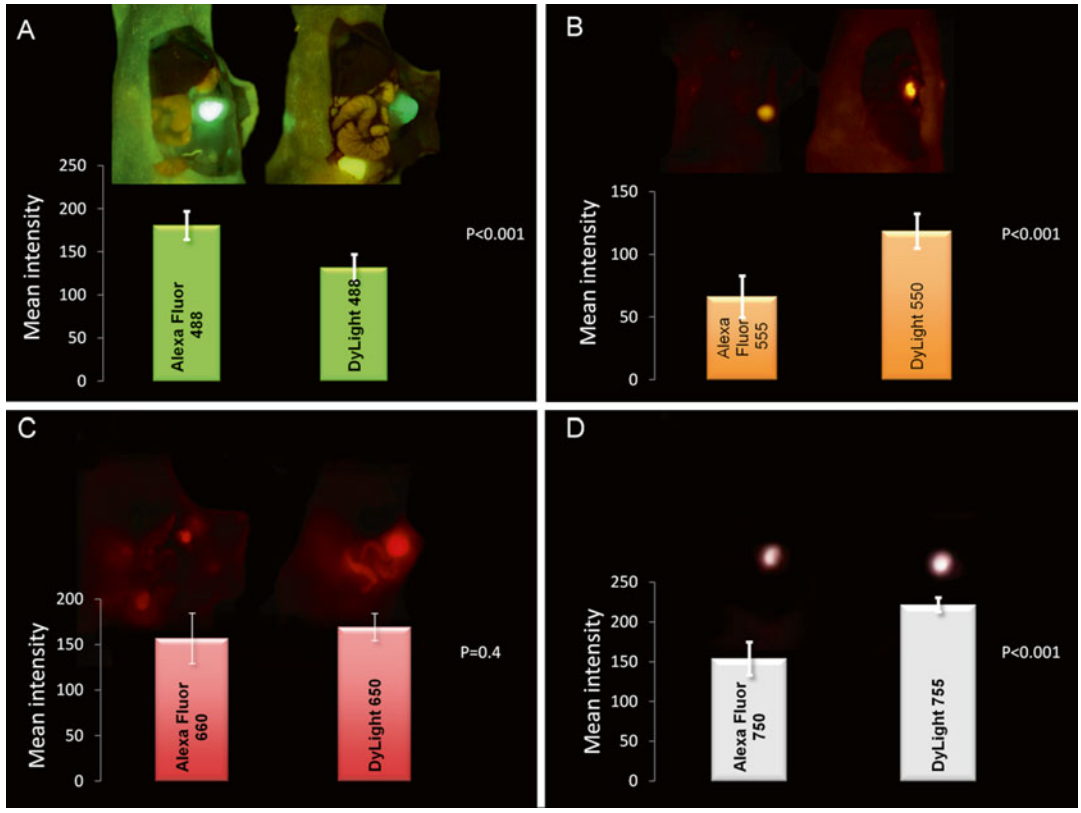

Fig. 22.10 Chimeric anti-CEA antibody conjugated with visible or near-infrared fluorescent dyes were used for imaging pancreatic cancer in orthotopic nude mouse models. (**a**) Alexa Fluor 488 was significantly brighter than DyLight 488 ($p<0.001$). (**b**) DyLight 550 was significantly brighter than Alexa Fluor 555 ($p<0.001$). (**c**) DyLight 650 was brighter than Alexa Fluor 660. (**d**) DyLight 755 was significantly brighter than Alexa Fluor 750 ($p<0.001$). There was decreasing ability to discern the background with increasing wavelength of the fluorophores (**a**–**d**) [14]

7. Robinson MH, Thomas WM, Hardcastle JD, Chamberlain J, Mangham CM. Change towards earlier stage at presentation of colorectal cancer. Br J Surg. 1993;80(12):1610–2.
8. Pawlik TM, Schulick RD, Choti MA. Expanding criteria for resectability of colorectal liver metastases. Oncologist. 2008;13(1):51–64.
9. Bonjer HJ, Hop WC, Nelson H, Sargent DJ, Lacy AM, Castells A, et al. Laparoscopically assisted vs open colectomy for colon cancer: a meta-analysis. Arch Surg. 2007;142(3):298–303.
10. Turrini O, Viret F, Guiramand J, Lelong B, Bege T, Delpero JR. Strategies for the treatment of synchronous liver metastasis. Eur J Surg Oncol. 2007;33(6):735–40.
11. Andreoni B, Chiappa A, Bertani E, Bellomi M, Orecchia R, Zampino M, et al. Surgical outcomes for colon and rectal cancer over a decade: results from a consecutive monocentric experience in 902 unselected patients. World J Surg Oncol. 2007;5:73.
12. Kaushal S, McElroy MK, Luiken GA, Talamini MA, Moossa AR, Hoffman RM, et al. Fluorophore-conjugated anti-CEA antibody for the intraoperative imaging of pancreatic and colorectal cancer. J Gastrointest Surg. 2008;12(11):1938–50.
13. McElroy M, Kaushal S, Luiken GA, Talamini MA, Moossa AR, Hoffman RM, et al. Imaging of primary and metastatic pancreatic cancer using a fluorophore-conjugated anti-CA19-9 antibody for surgical navigation. World J Surg. 2008;32(6):1057–66.
14. Maawy AA, Hiroshima Y, Kaushal S, Luiken GA, Hoffman RM, Bouvet M. Comparison of a chimeric anti-carcinoembryonic antigen antibody conjugated with visible or near-infrared fluorescent dyes for imaging pancreatic cancer in orthotopic nude mouse models. J Biomed Opt. 2013;18(12):126016.
15. Metildi CA, Kaushal S, Lee C, Hardamon CR, Snyder CS, Luiken GA, et al. An LED light source and novel fluorophore combinations improve fluorescence laparoscopic detection of metastatic pancreatic cancer in orthotopic mouse models. J Am Coll Surg. 2012; 214(6):997–1007.e2.

16. Metildi CA, Kaushal S, Luiken GA, Talamini MA, Hoffman RM, Bouvet M. Fluorescently labeled chimeric anti-CEA antibody improves detection and resection of human colon cancer in a patient-derived orthotopic xenograft (PDOX) nude mouse model. J Surg Oncol. 2014;109:451.
17. Metildi CA, Kaushal S, Pu M, Messer KS, Luiken GA, Moossa AR, et al. Fluorescence-guided surgery with a fluorophore-conjugated antibody to carcinoembryonic antigen (CEA) that highlights the tumor improves surgical resection and increases survival in orthotopic mouse models of human pancreatic cancer. Ann Surg Oncol. 2014;21:1405.
18. Tran Cao HS, Kaushal S, Metildi CA, Menen RS, Lee C, Snyder CS, et al. Tumor-specific fluorescence antibody imaging enables accurate staging laparoscopy in an orthotopic model of pancreatic cancer. Hepatogastroenterology. 2012;59(118):1994–9.
19. Gold P, Freedman SO. Demonstration of tumor-specific antigens in human colonic carcinomata by immunological tolerance and absorption techniques. J Exp Med. 1965;121:439–62.
20. Gold P, Shuster J, Freedman SO. Carcinoembryonic antigen (CEA) in clinical medicine: historical perspectives, pitfalls and projections. Cancer. 1978;42(3 Suppl):1399–405.
21. Gold P, Freedman SO. Specific carcinoembryonic antigens of the human digestive system. J Exp Med. 1965;122(3):467–81.
22. Albers GH, Fleuren G, Escribano MJ, Nap M. Immunohistochemistry of CEA in the human pancreas during development, in the adult, chronic pancreatitis, and pancreatic adenocarcinoma. Am J Clin Pathol. 1988;90(1):17–22.
23. Yamaguchi K, Enjoji M, Tsuneyoshi M. Pancreatoduodenal carcinoma: a clinicopathologic study of 304 patients and immunohistochemical observation for CEA and CA19-9. J Surg Oncol. 1991;47(3):148–54.
24. Prall F, Nollau P, Neumaier M, Haubeck HD, Drzeniek Z, Helmchen U, et al. CD66a (BGP), an adhesion molecule of the carcinoembryonic antigen family, is expressed in epithelium, endothelium, and myeloid cells in a wide range of normal human tissues. J Histochem Cytochem. 1996;44(1):35–41.
25. Nap M, Mollgard K, Burtin P, Fleuren GJ. Immunohistochemistry of carcino-embryonic antigen in the embryo, fetus and adult. Tumour Biol. 1988;9(2–3):145–53.
26. Fletcher RH. Carcinoembryonic antigen. Ann Intern Med. 1986;104(1):66–73.
27. Kammerer R, von Kleist S. CEA expression of colorectal adenocarcinomas is correlated with their resistance against LAK-cell lysis. Int J Cancer. 1994;57(3):341–7.
28. Locker GY, Hamilton S, Harris J, Jessup JM, Kemeny N, Macdonald JS, et al. ASCO 2006 update of recommendations for the use of tumor markers in gastrointestinal cancer. J Clin Oncol. 2006;24(33):5313–27.
29. Goldstein MJ, Mitchell EP. Carcinoembryonic antigen in the staging and follow-up of patients with colorectal cancer. Cancer Invest. 2005;23(4):338–51.
30. Fu XY, Besterman JM, Monosov A, Hoffman RM. Models of human metastatic colon cancer in nude mice orthotopically constructed by using histologically intact patient specimens. Proc Natl Acad Sci U S A. 1991;88(20):9345–9.
31. Kishimoto H, Maawy AA, Sato S, Murakami T, Uehara F, Miwa S, et al. Hand-held high-resolution fluorescence imaging system for fluorescence-guided surgery of patient and cell-line pancreatic tumors growing orthotopically in nude mice. J Surg Res. 2014;187:510.
32. Yamauchi K, Yang M, Jiang P, Xu M, Yamamoto N, Tsuchiya H, et al. Development of real-time subcellular dynamic multicolor imaging of cancer-cell trafficking in live mice with a variable-magnification whole-mouse imaging system. Cancer Res. 2006; 66(8):4208–14.
33. Nelson AL, Dhimolea E, Reichert JM. Development trends for human monoclonal antibody therapeutics. Nat Rev Drug Discov. 2010;9(10):767–74.
34. Metildi CA, Hoffman RM, Bouvet M. Fluorescence-guided surgery and fluorescence laparoscopy for gastrointestinal cancers in clinically-relevant mouse models. Gastroenterol Res Pract. 2013;2013:290634.